

^{17}O MQMAS NMR studies of zeolite HY

Luming Peng ^a, Hua Huo ^a, Zhehong Gan ^b, Clare P. Grey ^{a,*}

^a Department of Chemistry, State University of New York at Stony Brook, Stony Brook, NY 11794-3400, United States

^b National High Magnetic Field Laboratory, 1800 East Paul Dirac Drive, Tallahassee, FL 32310, United States

Received 4 April 2007; received in revised form 19 April 2007; accepted 19 April 2007

Available online 3 May 2007

Abstract

High-resolution ^{17}O multiple-quantum MAS (MQMAS) NMR spectra have been obtained for zeolite HY in order to study its local structure and Brønsted acidity. The ^{17}O NMR signals due to all the different oxygen environments have been observed in one single experiment, including the readily-resolved signals arising from the two types of oxygen atoms of the zeolite framework (Si–O–Al and Si–O–Si), and oxygen atoms directly bound to Brønsted acid sites (Si–O(H)–Al). The ^{17}O NMR parameters such as the isotropic chemical shift (δ_{CS}) and quadrupolar coupling parameters (quadrupolar coupling constant, QCC and asymmetry parameter, η) for these oxygen species have been extracted and found to be consistent with the results from previous NMR measurements. The NMR parameters of the framework sites reveal a greater distribution of T–O–T' bond angles over those typically observed in hydrated zeolites.

© 2007 Elsevier Inc. All rights reserved.

Keywords: ^{17}O ; MQMAS; NMR; Zeolite; HY

1. Introduction

Microporous zeolites have been widely used as catalysts in industry. The size and connectivity of the cages and channels of the zeolites' structure, along with their Brønsted or Lewis acidity, plays a critical role in controlling the activity and selectivity of these zeolite-based catalysts [1,2]. The oxygen atoms of the zeolite framework have the largest ionic radius among the typical atoms in zeolites, therefore they are expected to be intimately involved in adsorption and catalysis [3–5]. The NMR-active oxygen nucleus, ^{17}O , not only possesses a very large chemical shift range (>1000 ppm), but as a quadrupolar nucleus, is significantly affected by the electric field gradient (EFG) surrounding the nucleus [6]. Hence, ^{17}O MAS NMR spectroscopy is an extremely sensitive probe of local structure and ^{17}O NMR spectra of zeolites should, in principle, provide considerable information [7]. With the develop-

ments in high magnetic field strengths and fast magic angle spinning (MAS) NMR techniques, high resolution ^{17}O NMR spectra have now been collected for a variety of zeolites [8–13]. The resonance due to Si–O–Al and Si–O–Si sites in the zeolite framework, which overlap in the ^{17}O 1-pulse NMR spectra, can be readily distinguished in ^{17}O multiple-quantum MAS (MQMAS) NMR [8]. However, the resonance from the most catalytically relevant oxygen atoms, i.e., the ones which are directly bound to the Brønsted acid sites has been difficult to detect. Recently, we reported the direct observation of the ^{17}O signal from this site, by using $^{17}\text{O}/^1\text{H}$ double resonance NMR techniques [14,15]. However, in these experiments the resonances due to Si–OH–Al sites are selected and the resonances arising from Si–O–Al and Si–O–Si linkages are either not observed or very weak (e.g., in the cross-polarization experiment) or observed but still not well resolved (e.g., in a ^1H – ^{17}O REDOR experiment). Here, we demonstrate the application of ^{17}O MQMAS NMR spectroscopy to resolve the framework sites and the sites directly bound to Brønsted acid sites in zeolite HY (Fig. 1) in a single experiment. The NMR parameters

* Corresponding author. Tel.: +1 631 632 9548; fax: +1 631 632 5731.
E-mail address: cgrey@notes.cc.sunysb.edu (C.P. Grey).

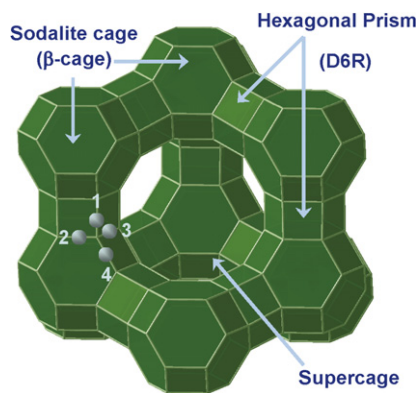


Fig. 1. Structure of zeolite HY and the positions of the four crystallographically distinct oxygen sites. The Brønsted acid sites have been located, by using diffraction methods, in both the super- and sodalite cages of HY.

extracted in this study are discussed in terms of their local environments.

2. Experimental section

2.1. Materials preparation

Acidic zeolites are susceptible to dealumination, particularly on heat-treatment of the hydrated samples, thus, ^{17}O -enriched zeolite HY was prepared via the ^{17}O -enriched, sodium-exchanged form of the zeolite [15]. NaY ($n(\text{Si})/n(\text{Al})$ ratio of 2.6; Strem Chemicals) was dehydrated at 773 K for 12 h and then ^{17}O enriched by heating in $^{17}\text{O}_2$ gas (59.6% enriched $^{17}\text{O}_2$; Isotec, Inc.) at 853 K for 12 h [13]. ^{17}O -enriched zeolite NH_4Y was prepared from NaY by ion exchange with a 1 M NH_4NO_3 solution at ambient temperature for 12 h (repeated 5 times). In order to obtain zeolite HY, ^{17}O -enriched NH_4Y was then slowly heated under vacuum ($<1 \times 10^{-2}$ Torr) from room temperature to 383 K in 7 h, and then to 673 K in 12 h where the temperature was held at 673 K for a further 12 h. The sample was kept and packed in the N_2 glove box prior to the NMR experiments.

3. Solid-state NMR spectroscopy

MAS NMR spectra were obtained with Bruker Avance 600 and 833 MHz spectrometers, with 89 mm wide-bore 14.1 T and 31 mm ultra-narrow-bore 19.4 T superconducting magnets, respectively, in 4 mm rotors. Rotor caps with o-rings were used to avoid the adsorption of water during the NMR measurements. ^{17}O chemical shifts are referenced to H_2O at 0.0 ppm. A standard triple-quantum MAS pulse sequence with two hard pulses followed by a z-filter was used. In the experiment performed at 14.1 T, two-pulse phase modulated (TPPM) [16] decoupling was applied during t_1 -evolution and t_2 -acquisition. The optimized parameters for the MQMAS experiments were set by using the ^{17}O -enriched zeolite HY sample. NMR line shape simula-

tions were performed with the Wsolids package developed by Eichele and Wasylishen [17].

4. Results and discussion

The two-dimensional (2-D) ^{17}O MQMAS NMR (with ^1H decoupling) spectrum of zeolite HY and its F_1/F_2 projection acquired at a magnetic strength of 14.1 T are shown in Fig. 2a. Similar to the 1-pulse ^{17}O MAS NMR data, the anisotropic projection of the MQMAS spectrum shows one broad resonance ($\delta_2 = 50$ to -50) with a maximum at $\delta_2 = 20$ and a small shoulder centered at $\delta_2 = -25$ ppm [15], where δ_2 is the center of gravity of the resonance in the anisotropic (F_2) dimension. The isotropic (F_1) projec-

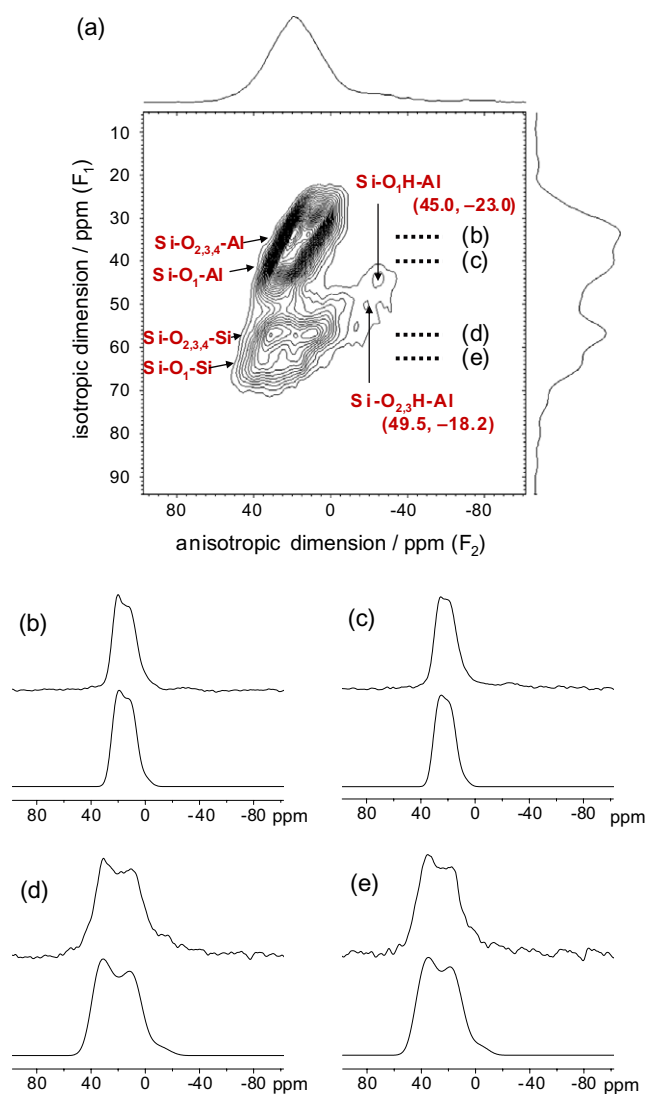


Fig. 2. ^{17}O MQMAS NMR spectra of HY at 14.1 T. (a) 2-D MQMAS spectrum. Spinning speed: 13 kHz, recycle delay: 1 s. The projections of F_2 and F_1 dimensions are shown on the above and right side of the 2-D-spectrum, respectively. (b)–(e): Slices of anisotropic dimension at 35.1, 40.0, 57.2 and 63.0 ppm in F_1 dimension (top), and the simulations of the spectra (bottom). Simulation parameters are given in Tables 1 and 2. The dotted lines in the 2-D spectrum show where the slices are taken.

tion, however, shows four resonances with centers of gravity, δ_1 of 35.1, 40.0, 57.2 and 63.0 ppm, which can be assigned to framework oxygen sites in Si–O–Al (35.1 and 40.0 ppm) and Si–O–Si (57.2 and 63.0 ppm) linkages, respectively. The NMR parameters for the Si–O–Si and Si–O–Al linkages were therefore extracted by simulating the slices of the F_2 dimension (Fig. 2b–e) and the parameters (quadrupolar coupling constants, QCC, asymmetry parameter, η , and chemical shift, δ_{CS}) are listed in Table 1.

Previous crystallographic studies have shown that the T–O–T (T = Si or Al) bond angles for the four crystallographically distinct oxygen sites in faujasite type zeolites (Fig. 1) generally increase in the order $O_1 < O_3 < O_2 < O_4$ [10,18,19], while the MQMAS [11] and double rotation (DOR) [12] NMR results indicate there is a linear correlation with a negative linear coefficient between the ^{17}O isotropic chemical shift and T–O–T bond angle for structurally similar local environments. Thus the ^{17}O chemical shifts should follow the order $O_1 > O_3 > O_2 > O_4$. Although the intensities in the MQMAS spectra are sensitive to the size of the quadrupolar product, P_Q , it is still possible to compare the relative intensities of the resonances, if the range in the values of P_Q is small, which is the case for different bare oxygen framework sites. The intensity ratio of the two resonances corresponding to Si–O–Si environments at $\delta_1 = 57.2$ and 63.0 ppm is close to 3:1. Thus, according to the values of δ_{CS} obtained from the simulations (Table 1), these two resonances are assigned to Si–O_{2,3,4}–Si and Si–O₁–Si, respectively, where the O₁ and O₄ sites point into the supercage and the O₂ and O₃ into the sodalite cages. Similarly, the resonances arising from Si–O–Al sites at $\delta_1 = 35.1$ and $\delta_1 =$

40.0 ppm are assigned to Si–O_{2,3,4}–Al and Si–O₁–Al, respectively.

The shifts δ_1 and δ_2 , can be used to extract the values for isotropic chemical shift, δ_{CS} , and P_Q , directly, without simulating the F_2 dimension. For a $I = 5/2$ nucleus these parameters are given by:

$$\delta_{CS} = (17/27)\delta_1 + (10/27)\delta_2, \quad (1)$$

$$P_Q = 0.04\nu_0(85(\delta_1 - \delta_2)/1296)^{1/2}, \quad (2)$$

and the expression for P_Q :

$$P_Q = \text{QCC}(1 + \eta^2/3)^{1/2}, \quad (3)$$

where ν_0 , QCC and η are the carrier frequency, the quadrupolar coupling constant and the asymmetry parameter, respectively. Conversely, the values of δ_1 and δ_2 can be predicted if δ_{CS} and P_Q are known. Since no strong peaks were seen for the resonances due to the oxygen atoms bound to Brønsted acid sites, their resonant frequencies were predicted from the NMR parameters obtained previously from $^1\text{H}/^{17}\text{O}$ two-dimensional HETCOR NMR spectroscopy in order to help locate these resonance [14]. Two resonances are predicted at $(\delta_1, \delta_2) = (50.0, -20.3)$ and $(46.6, -22.5)$ (Table 2), for the two different Brønsted acid oxygen sites. Therefore, the broad resonances with two maxima at $(\delta_1, \delta_2) = (49.5, -18.2)$ and $(45.0, -23.0)$ can be

Table 1
 ^{17}O NMR parameters and the observed/calculated NMR shifts for oxygen atoms in Si–O–Al and Si–O–Si environments at 14.1 and 19.4 T in zeolite HY

	Si–O _{2,3,4} –Al	Si–O ₁ –Al	Si–O _{2,3,4} –Si	Si–O ₁ –Si
QCC/MHz	3.7	3.5	5.3	5.1
η	0.2	0.3	0.1	0.3
δ_{CS}	27.5	33.3	44.0	50.0
14.1 T				
δ_1 (Cal.)	34.9	40.0	59.0	64.3
δ_1 (Exp.)	35.1	40.0	57.2	63.0
δ_2 (Cal.)	14.9	21.9	18.5	25.7
δ_2 (Exp.)	16.0	22.5	17.8	26.0
19.4 T				
δ_1 (Cal.)	31.9	36.8	51.9	57.5
δ_1 (Exp.)	31.0	36.9	51.8	57.5
δ_2 (Cal.)	20.9	27.3	30.6	37.3
δ_2 (Exp.)	21.6	27.9	31.0	37.9

The NMR parameters were obtained by fitting the slices of the anisotropic dimension at δ_1 (Exp.); they were used to calculate the shifts of the center of gravity in the F_2 and F_1 dimensions (δ_2 (Cal.) and δ_1 (Cal.)), from Eqs. (2) and (3). Estimated errors here and in Table 2 are ± 0.1 MHz for the QCC, ± 0.1 in η and ± 2 ppm in δ_{CS} for the data obtained at 14.1 T; and ± 0.1 MHz in QCC, ± 0.1 in η and ± 1 ppm in δ_{CS} for the data obtained at 19.4 T.

Table 2
 ^{17}O NMR parameters and the observed/calculated NMR shifts for oxygen atoms in Si–OH–Al environments at 14.1 T and 19.4 T in zeolite HY

	Si–O _{2,3} (H)–Al	Si–O ₁ (H)–Al
QCC/MHz ^a	6.2	6.0
η^a	0.9	1.0
δ_{CS}^a	24.0	21.0
14.1 T		
δ_1 (Cal.)	50.0	46.6
δ_2 (Cal.)	–20.3	–22.5
QCC (MHz) ^b	6.09	5.95
δ_{CS}^b	24.4	19.8
P_Q (MHz) ^b	6.86	6.87
δ_1 (Exp.)	49.5	45.0
δ_2 (Exp.)	–18.2	–23.0
19.4 T		
δ_1 (Cal.)	37.6	34.4
δ_2 (Cal.)	0.8	–1.8
QCC (MHz) ^b	6.23	5.95
δ_{CS}^b	23.5	20.9
P_Q (MHz) ^b	7.02	6.87
δ_1 (Exp.)	37.3	34.1
δ_2 (Exp.)	0.1	–1.5
QCC (MHz) ^c	6.16	5.95
δ_{CS}^c	24.0	20.4

^a NMR parameters are taken from Ref. [14] and were used to predict the resonant frequencies δ_1 (Cal.) and δ_2 (Cal.).

^b The NMR parameters were calculated from the observed shifts of center of gravity of the resonances (δ_1 (Exp.) and δ_2 (Exp.)) and η^a by using Eqs. (1)–(3).

^c The average values of NMR parameters obtained in this study.

tentatively assigned to oxygen atoms bound to Brønsted acid sites pointing to the sodalite cages and supercages, respectively. These resonances are not well resolved from the resonances due to the framework oxygen atoms. Simulation attempts for the slices of anisotropic dimension corresponding to the two Brønsted acid sites (not shown) failed because the slices show only a broad peak with a poorly defined second-order quadrupolar line shape. The values of δ_{CS} calculated from the observed shifts are 24.4 and 19.8 ppm, for the two resonances at $(\delta_1, \delta_2 \text{ (ppm)}) = (49.5, -18.2)$ and $(45.0, -23.0)$, respectively (Table 2), which are very similar to the results from our previous ^1H – ^{17}O HETCOR NMR spectra of the same sample, where values of δ_{CS} are 24.0 and 21.0 ppm for these two resonances were obtained [14]. Determination of a QCC from δ_1 and δ_2 requires the value of asymmetry parameter η , which cannot be obtained from line shape simulation here due to low S/N . Therefore, the values of η extracted from the HETCOR NMR spectra [14] (Table 2) for the two Brønsted acid sites, which are also in agreement with the results from the ab-initio calculations [15], were used here in order to predict the QCCs.

The most important line broadening factor in these experiments, the second-order quadrupole interaction is inversely proportional to the magnetic field strength. Hence, to obtain better resolution, especially for the Brønsted acid oxygen sites, which possess much larger QCCs, ^{17}O MQMAS NMR data were collected at an ultra-high magnetic field strength of 19.4 T (Fig. 3a). To maximize the sample volume and gain the highest power for the multiple-quantum excitation pulses, a single channel 4 mm probe was used in this experiment. Again, both the signals due to Si–O–Al and Si–O–Si sites can be divided in two main groups. Line shape simulations were performed to extract their NMR parameters (Fig. 3b–e, simulation results are listed in Table 1). The results are consistent with the 14.1 T data, and the two groups are assigned to O_1 , and $\text{O}_{2,3,4}$, according to their chemical shifts. It is clear that this interpretation is too simplistic: a distribution in chemical shifts for both the Si–O–Si and Si–O–Al local environments is seen, as manifested by the spreading of the resonances along the isotropic chemical shift direction (in the MQMAS NMR experiment, this is not simply aligned along F_1 or F_2 [20], but along the direction indicated in Fig. 3). The distribution in chemical shifts has increased noticeably over that obtained for both hydrated NH_4Y and NaY zeolites, reflecting an increased range in distributions of Si–O–Al bond angles on both protonation and dehydration. For example, the range of isotropic ^{17}O chemical shifts (in Si–O–Al) seen here for dehydrated HY of 22–42 ppm, corresponds to a range of bond angles from 143° to 172° based on the correlation of chemical shifts and Si–O–Al angles ($\delta/\text{ppm} = -0.65\alpha/^\circ + 134$) or ($\delta/\text{ppm} = -0.71\alpha/^\circ + 143.7$), obtained in low silicate zeolites [11,12]. In contrast, the bond angles for hydrated NaY , calculated by using the same chemical shift/bond angle correlation vary from 142° to 154° (Si–

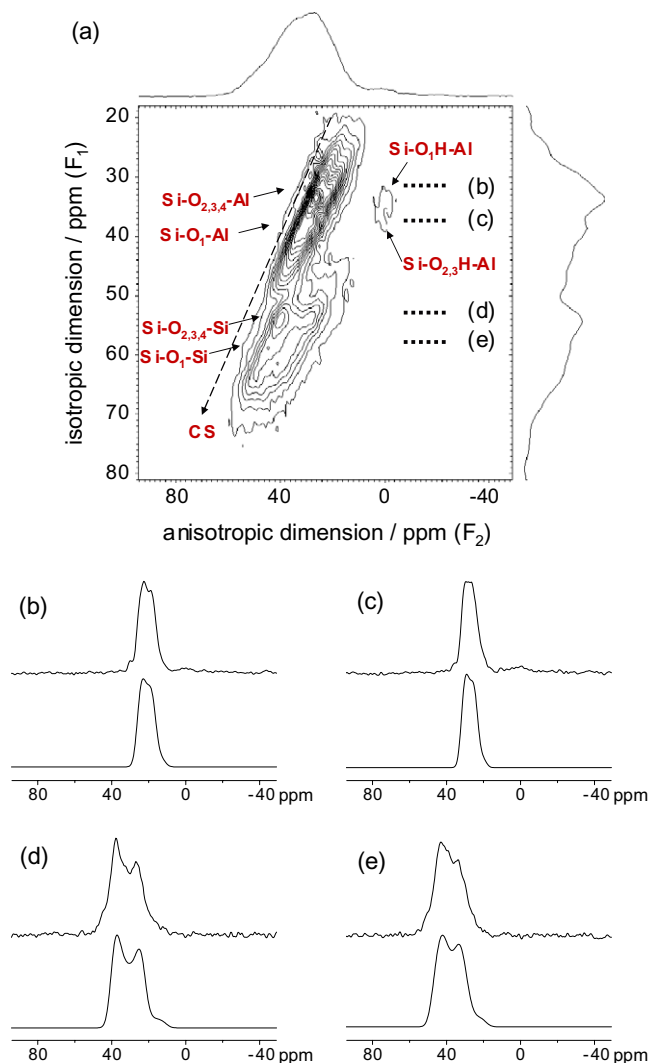


Fig. 3. ^{17}O MQMAS NMR spectra of HY at 19.4 T. (a) 2-D MQMAS spectrum. Spinning speed: 10 kHz, recycle delay: 0.5 s. The projections of F_2 and F_1 dimensions are shown on the above and right side of the 2-D spectrum, respectively. The dashed arrow shows the direction of the chemical shift. (b)–(e): Slices of anisotropic dimension at 31.0, 36.9, 51.8 and 57.5 ppm in the F_1 dimension (top), and the corresponding simulations (bottom). Simulation parameters are given in Tables 1 and 2. The dotted lines in 2-D spectra show where the slices are taken.

O–Al), while those for dehydrated and hydrated NH_4Y vary from 144° to 157° and 136° to 151° , respectively [21].

The predicted NMR shifts (in ppm) for the resonances due to Brønsted acid sites are $(\delta_1, \delta_2) = (37.6, 0.8)$ and $(34.4, -1.8)$ (Table 2). This agrees with the two maxima $((37.3, 0.1)$ and $(34.1, -1.5))$ seen for the broad peaks in the MQMAS spectrum, therefore, these two resonances are tentatively assigned to the sodalite and supercage Brønsted acid sites, respectively. Using the observed shifts (δ_1, δ_2) at 19.4 T and η obtained from the HETCOR NMR spectrum, QCC and δ_{CS} have been calculated and shown in Table 2, and the average NMR parameters and the average of the two sets of parameters obtained in this MQMAS study at the two different fields (14.1 T and 19.4 T) are

given in the end of Table 2. The extracted QCC for oxygen atoms directly bound to Brønsted acid sites pointing into the sodalite cages (sites O₂ and O₃) is only slightly larger than the QCC determined for the oxygen atoms bound to Brønsted acid sites in supercages (O₁; no proton atoms were found bound to the O₄ site in previous neutron diffraction studies [18]). Both values are slightly smaller than the results determined by HETCOR NMR spectroscopy [14]. Although the signal intensities in MQMAS spectrum are still very low, the summation of the slices of anisotropic dimension at δ_1 from 30 to 40 ppm shows an intense resonance, corresponding to the Si–O–Al sites, with an associated weaker resonance, which has a characteristic line shape due to second-order quadrupolar interaction with a large η (Fig. 4a). This lineshape was simulated by using the NMR parameters given in the end of Table 2 (i.e., the parameters representing the average of the values determined at the two fields). A good fit was achieved with NMR parameters obtained for the sodalite (O₂ and O₃) Brønsted acid sites (solid line in Fig. 4b), while the overall lineshape calculated by using the NMR parameters of the O₁ site in the supercage occurs at a slightly more negative frequency (dashed line in Fig. 4b), than the experimental spectrum. However, the signal-to-noise of this experiment does not justify further simulations of the resonance. These calculations and simulations, in combination with the 14.1 T data, confirm our assignments of these resonances to the Brønsted acid oxygen atoms.

The oxygen atoms directly bound to Brønsted acid sites possess the largest QCCs and η s in the structure. In addition, the directly bonded O–H distance is very short (0.98–1.01 Å [14]) thus a large ¹H–¹⁷O heteronuclear dipolar coupling (>15 kHz) is present. During the first evolution period in the MQMAS experiments, the ¹⁷O spins

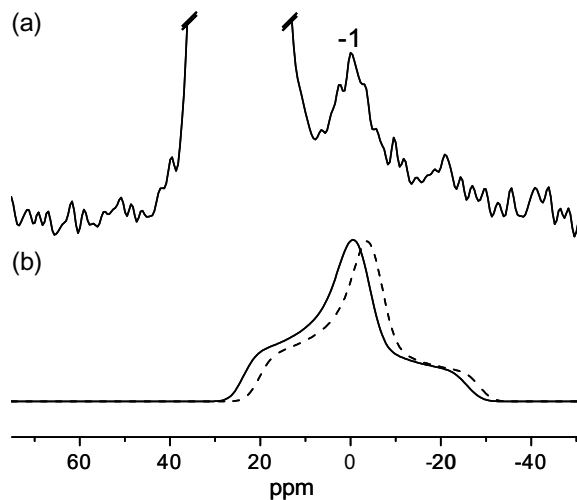


Fig. 4. Summation of the slices of F_2 dimension from 30 to 40 ppm in F_1 dimension of the 19.4 T MQMAS data (a), in comparison with simulations (b). Simulation parameters are QCC = 6.16 MHz, $\eta = 0.9$ and $\delta_{CS} = 24.0$ for O_{2,3} (solid line) and QCC = 5.95 MHz, $\eta = 1.0$ and $\delta_{CS} = 20.4$ for O₁ (dashed line).

evolve in a triple-quantum coherence, thus the size of the dipolar interaction between the ¹⁷O and ¹H nuclei is three times larger than the dipolar interaction for a single-quantum coherence (i.e., following a simple $\pi/2$ pulse). MQMAS NMR is an echo experiment and this huge dipolar coupling (50–60 kHz), in combination with large QCC for the Brønsted acid site, must prevent effective refocusing at the echo, resulting in a considerably reduced intensity for the sites nearby protons. A similar phenomenon was seen in the previous work of Massiot and coworkers [22] on materials with directly bound Al and F atoms, and thus with large ²⁷Al–¹⁹F dipolar couplings. They observed that standard decoupling methods (i.e., CW decoupling) were not sufficient, and TPPM decoupling methods, which result in more effective decoupling, were required in their systems in order to obtain ²⁷Al MQMAS NMR spectra with improved signal-to-noise ratios. Motion associated with the Brønsted acid sites, as observed in our previous ¹H and ¹⁷O NMR spectra [14], may also contribute to the loss of intensity of the MQMAS resonances of these sites. Finally, the 3Q transition will be difficult to excite, due to the large QCCs and dipolar couplings. While our results show that data obtained at high magnetic field strength (19.4 T) showed more characteristic and well resolved line shapes, as compared to the lower field (14.1 T) data, only a single channel NMR probe was available to us at high fields, and no decoupling could be performed. Unfortunately, the construction of a double resonance probe for use at high fields often involves compromising either on the power on the X channel (which should be maximized for efficient 3Q excitation) or on the power on the H channel, (which should be maximized for efficient decoupling).

The values of ¹⁷O NMR parameters are found to be very distinct for the different oxygen species, which makes the ¹⁷O MQMAS NMR spectroscopy a very sensitive method for probing the environments of all of the oxygen species. Generally, the value of δ_{CS} increases in the order: Si–OH–Al < Si–O–Al < Si–O–Si. For different crystallographic oxygen sites in Si–O–Al and Si–O–Si environments, the O₁ site can be separated from the O₂, O₃, and O₄ in the MQMAS spectra, where the assignments made above were made based on previous NMR results that suggested that the oxygen sites with smaller T–O–T bond angles (O₁ < O₃ < O₂ < O₄) [19,23–25] show more positive values of δ_{CS} (O₁ > O₃ > O₂ > O₄) [11,12]. However, the values of δ_{CS} for the Brønsted acid sites do not follow this trend: O₁ bound to a proton is associated with a *slightly* more negative shift as compared to the O₂ and O₃ sites bound to protons. The assignment of these ¹⁷O resonances does not appear to be controversial, as it was made based on the ¹H–¹⁷O HETCOR NMR [14], i.e., the O₁ ¹⁷O was associated with a ¹H resonance at 3.9 ppm, due to protons in the supercage, while the O₂/O₃ resonances were associated with ¹H resonances at approx. 4.6 ppm due to sites in the sodalite cages. Furthermore, the distribution of chemical shifts for the Brønsted acid sites is smaller than that seen for the framework sites. The decrease in chemical

shift distribution likely reflect distortions to the Si–O(H)–Al bond angles that will occur on H⁺ binding to a bare Si–O–Al framework site, and it would appear that the range in bond-angles of the protonated sites is smaller than that observed for the four bare O sites. The isotropic chemical shifts should also be sensitive to the O–H bond lengths, but we note that since O–H bond lengths depend, at least to some degree on both the bond angles and the extent of H-bonding of the Brønsted proton to any nearby framework atoms, it is non-trivial to separate these different contributions, without studying a wider range of zeolitic systems. The size of QCC follows the order: Si–O–Al < Si–O–Si < Si–OH–Al. O₁ has a noticeably smaller QCC than that of O₂, O₃ and O₄, in both Si–O–Si and Si–O–Al environments, which is consistent with the trends obtained from ab-initio calculations for Si–O–Si [26–28] and Si–O–Al [28] linkages and experimental data for Si–O–Si sites in SiO₂ polymorph coesite [4], where smaller T–O–T angles gave rise to smaller QCCs. The observation a correlation between the QCC and the T–O–T' angle provides further support for our earlier assignments of the peaks to different framework sites, based on the correlations involving the chemical shift. The QCC of O₁ in the Si–O₁(H)–Al linkage is slightly smaller than that of for O₂ and O₃, consistent with the smaller bond angle for the bare site. Both the values of η at Si–O–Al and Si–O–Si sites are in the same range (0.1–0.3), but they are much smaller than η at Si–OH–Al sites, which is close to 1. Site O₁ has larger η than sites O₂, O₃ and O₄ in Si–O–Al, Si–O–Si and Si–OH–Al linkages.

5. Conclusions

Signals arising from Si–O–Al, Si–O–Si and Si–OH–Al sites can be detected simultaneously in the ¹⁷O MQMAS NMR spectrum of zeolite HY. Due to the distinct NMR parameters possessed by the three different oxygen species, these signals can be well resolved in the MQMAS spectra. The QCCs and η s of Si–OH–Al sites are significantly larger than those of the Si–O–Al and Si–O–Si sites, which, in combination with the large dipolar coupling of these sites to the nearby protons, leads to a reduction in the intensities of the MQMAS signals from this site, in comparison to the those of the framework sites.

The ¹⁷O signals from the O₁ and O_{2,4} in both Si–O–Al and Si–O–Si linkages can be distinguished in the MQMAS spectrum. The resonances from O₁ and O_{2,3} sites in the Si–OH–Al linkages can also be separated. The two sets of NMR parameters extracted for the Brønsted acid sites are very similar and are consistent with our results obtained in ¹H–¹⁷O HETCOR NMR experiments. Acquisition of the MQMAS data at high magnetic field strengths (19.4 T) reduced the second-order quadrupolar interactions and resulted in more clearly resolved ¹⁷O signals due to Brønsted acid sites; however, the sensitivity of this experiment could most likely be improved further over that achieved in this work via the use of ¹H decoupling schemes

during triple-quantum evolution and single-quantum acquisition. The results presented in this study show that ¹⁷O MQMAS NMR spectroscopy can probe both framework and Brønsted acid oxygen sites in zeolite catalysts at the same time allowing the various NMR parameters to be extracted. Since oxygen atoms are intimately involved in gas sorption, ¹⁷O MQMAS NMR spectroscopy provides a powerful probe to investigate sorption and catalysis processes and to develop structure–function relationships of catalysts.

Acknowledgment

We thank Dr. Martine Ziliox for her help in obtaining the 14.1 T NMR data. Financial support was provided by the DOE via grant DEFG0296ER14681.

References

- [1] A. Corma, *Chem. Rev.* 95 (1995) 559.
- [2] H.G. Karge, M. Hunger, H.K. Beyer, in: J. Weitkamp, L. Puppe (Eds.), *Catalysis and Zeolites: Fundamentals and Applications*, Springer, New York, 1999, p. 198.
- [3] L.M. Bull, A.K. Cheetham, *Stud. Surf. Sci. Catal.* 105 (1997) 471.
- [4] P.J. Grandinetti, J.H. Baltisberger, I. Farnan, J.F. Stebbins, U. Werner, A. Pines, *J. Phys. Chem.* 99 (1995) 12341.
- [5] K.T. Mueller, Y. Wu, B.F. Chmelka, J. Stebbins, A. Pines, *J. Am. Chem. Soc.* 113 (1991) 32.
- [6] C.P. Grey, in: S.M. Auerbach, K.A. Carrado, P.K. Dutta (Eds.), *Handbook of Zeolite Science and Technology*, Marcel Dekker, 2003, p. 205.
- [7] M. Profeta, F. Mauri, C.J. Pickard, *J. Am. Chem. Soc.* 125 (2003) 541.
- [8] J.P. Amoureux, F. Bauer, H. Ernst, C. Fernandez, D. Freude, D. Michel, U.T. Pingel, *Chem. Phys. Lett.* 285 (1998) 10.
- [9] L.M. Bull, B. Bussemer, T. Anupold, A. Reinhold, A. Samoson, J. Sauer, A.K. Cheetham, R. Dupree, *J. Am. Chem. Soc.* 122 (2000) 4948.
- [10] L.M. Bull, A.K. Cheetham, T. Anupold, A. Reinhold, A. Samoson, J. Sauer, B. Bussemer, Y. Lee, S. Gann, J. Shore, A. Pines, R. Dupree, *J. Am. Chem. Soc.* 120 (1998) 3510.
- [11] D. Freude, T. Loeser, D. Michel, U. Pingel, D. Prochnow, *Solid State Nucl. Magn. Reson.* 20 (2001) 46.
- [12] U.T. Pingel, J.P. Amoureux, T. Anupold, F. Bauer, H. Ernst, C. Fernandez, D. Freude, A. Samoson, *Chem. Phys. Lett.* 294 (1998) 345.
- [13] J.E. Readman, N. Kim, M. Ziliox, C.P. Grey, *Chem. Commun.* (2002) 2808.
- [14] L. Peng, H. Huo, Y. Liu, C.P. Grey, *J. Am. Chem. Soc.* 129 (2007) 335.
- [15] L. Peng, Y. Liu, N. Kim, J.E. Readman, C.P. Grey, *Nature Mater.* 4 (2005) 216.
- [16] A.E. Bennett, C.M. Rienstra, M. Auger, K.V. Lakshmi, R.G. Griffin, *J. Chem. Phys.* 103 (1995) 6951.
- [17] K. Eichele, R.E. Wasylshen, *WSolids1 ver. 1.17.30*, Dalhousie University, Halifax, Canada, 2001.
- [18] M. Czjzek, H. Jobic, A.N. Fitch, T. Vogt, *J. Phys. Chem.* 96 (1992) 1535.
- [19] F. Porcher, M. Souhassou, Y. Dusausoy, C. Lecomte, *Eur. J. Miner.* 11 (1999) 333.
- [20] J.P. Amoureux, C. Fernandez, *Solid State Nucl. Magn. Reson.* 10 (1998) 211.
- [21] L. Peng, J.E. Readman, N. Kim, C.P. Grey, O-17 solid state NMR studies of faujasite type zeolites, in: *Proc. of the abstracts of Papers of*

- the American Chemical Society. American Chemical Society, New Orleans, 2003.
- [22] V. Lacassagne, P. Florian, V. Montouillout, C. Gervais, F. Babonneau, D. Massiot, *Magn. Reson. Chem.* 36 (1998) 956.
- [23] A.N. Fitch, H. Jovic, A. Renouprez, *J. Phys. Chem.* 90 (1986) 1311.
- [24] J.A. Hriljac, M.M. Eddy, A.K. Cheetham, J.A. Donohue, G.J. Ray, *J. Solid State Chem.* 106 (1993) 66.
- [25] Y.J. Lee, S.W. Carr, J.B. Parise, *Chem. Mater.* 10 (1998) 2561.
- [26] T.M. Clark, P.J. Grandinetti, *Solid State Nucl. Magn. Reson.* 27 (2005) 233.
- [27] X. Xue, M. Kanzaki, *Phys. Chem. Miner.* 26 (1998) 14.
- [28] X.Y. Xue, M. Kanzaki, *J. Phys. Chem. B* 103 (1999) 10816.